Chinese Physics Letters

LETTER

# Ergotropy in Quantum Batteries

Cite as: Cheng-Jie Wang *et al*. 2026 *Chin. Phys. Lett.* **43** 060602

DOI CSTR

## Recommended Articles

**Thermal Management of Air-Cooling Lithium-Ion Battery Pack**
Jianglong Du, Haolan Tao, Yuxin Chen, Xiaodong Yuan, Cheng Lian, and Honglai Liu
*Chin. Phys. Lett.* **38**, 118201 (2021)

**A 700 Whkg$^{-1}$ Rechargeable Pouch Type Lithium Battery**
Quan Li, Yang Yang, Xiqian Yu, and Hong Li
*Chin. Phys. Lett.* **40**, (2023)

**Lithium Ion Batteries Operated at –100 °C**
Jianli Gai, Jirong Yang, Wei Yang, Quan Li, Xiaodong Wu, and Hong Li
*Chin. Phys. Lett.* **40**, (2023)

**Multi-Scale X-Ray Imaging Technologies for Rechargeable Batteries**
Zihan Xu, Hanwen An, and Jiajun Wang
*Chin. Phys. Lett.* **41**, (2024)

**Compression of Battery X-Ray Tomography Data with Machine Learning**
Zipei Yan, Qiyu Wang, Xiqian Yu, Jizhou Li, and Michael K.-P. Ng
*Chin. Phys. Lett.* **41**, (2024)

iopscience.iop.org/cpl | cpl.iphy.ac.cn

A series journal of Chinese Physical Society distributed by IOP Publishing

Chinese Physics Letters

*Chin. Phys. Lett.* **43** 060602 (2026)

LETTER

DOI: 10.1088/0256-307X/43/6/060602
CSTR: 32039.14.0256-307X.43.6.060602

# Ergotropy in Quantum Batteries

**Cheng-Jie Wang(王成杰)[1] and Fu-Quan Dou(豆福全)[1,2,*]**

[1]College of Physics and Electronic Engineering, Northwest Normal University, Lanzhou 730070, China
[2]Gansu Provincial Research Center for Basic Disciplines of Quantum Physics, Lanzhou 730000, China

[*]Corresponding author. Email: doufq@nwnu.edu.cn

**Ergotropy, as a key figure of merit for the performance of quantum batteries (QBs), plays a crucial role in characterizing energy storage and extractable work. However, the dynamics and physical mechanisms governing ergotropy evolution remain to be fully understood. Here, we investigate the ergotropy of a general QB model and find that the charging process is accompanied by the variation and inversion of the energy level populations. In the absence of population inversion, the ergotropy is fully consistent with coherent ergotropy; in local and global population inversion, it is determined by both coherent and incoherent ergotropy. Via random sampling of quantum states and Hamiltonians, we show that coherence and the participation ratio enhance coherent ergotropy, whereas incoherent ergotropy–whether enhanced, unchanged, or suppressed–depends on diagonal entropy, the participation ratio, and energy level population ordering. We demonstrate that the ergotropy lower bound is incoherent ergotropy, the upper bound is the QB stored energy, and enhanced QB purity suppresses locked energy and boosts charging efficiency. Furthermore, we use the Tavis-Cummings (TC) and Jaynes-Cummings (JC) batteries as paradigms to validate our findings. Our work elucidates ergotropy underlying mechanisms in general QBs and establishes a rigorous framework for optimizing ergotropy and charging efficiency, paving the way for high-performance quantum energy-storage devices.**

## Introduction

Quantum thermodynamics focuses on the thermodynamic behavior of quantum systems, including energy conversion, work extraction, and the role of quantum resources such as quantum coherence [1–4] and entanglement [5–8]. Due to the constraints imposed by the second law of thermodynamics, the stored energy in the quantum system cannot be fully extracted [9,10]. The ergotropy [11], the maximum energy that can be extracted from a quantum system through cyclic unitary transformations, becomes one of the central issues of quantum thermodynamics [12]. Several appropriate characterizations of extractable work have been proposed, such as local work extraction, extended local ergotropy, and the free-energy difference [13,14]. These characterizations provide a framework to assess the impact of quantum resources, revealing that correlations induce suppression while coherence leads to enhancement in extractable work [15–17].

Quantum batteries (QBs)–one of the significant topics of quantum thermodynamics–are energy storage and extraction systems that utilize quantum mechanical principles to enhance performance or functionality [18–21]. Considerable efforts has focused on constructing QBs models [22–51], analyzing and optimizing their performance [52–66], and investigating the role of quantum resources [67–75]. The ergotropy is a vital figure of merit in QBs. Previous works have shown that quantum resources significantly affect the ergotropy, with coherence generally enhancing ergotropy whereas entanglement tends to suppress ergotropy [18,72,74,76–89]. Further theoretical and experimental investigations have demonstrated that ergotropy consists of both coherent and incoherent contributions and that the coherent ergotropy can be promoted by coherence [16,17,81,90]. Improving the ratio of coherent ergotropy to total ergotropy can mitigate self-discharging during the storage process, thereby enhancing the anti-aging capability of QBs [91]. The bounds of ergotropy are closely related to the battery capacity, and are determined by von Neumann's trace inequality [92,93]. Another performance metric is the charging efficiency, defined as the ratio between the ergotropy and the stored energy [88]. The higher-energy chargers and larger ensembles of battery units can improve this efficiency [19,31,56,74,94,95]. Nevertheless, these results are typically model dependent. Within a universal framework of QBs, the dynamical evolution of ergotropy (including coherent and incoherent ergotropy), their bounds, and the underlying physical mechanisms remain challenges. Therefore, it is of fundamental importance to address thoroughly the following issues: (i) How do coherent and incoherent ergotropy govern the ergotropy? (ii) How are coherent and incoherent ergotropy influenced by quantum resources, and how can one characterize the bounds of the ergotropy, in particular those of the coherent contribution? (iii) How do factors affect the charging efficiency, and how can this efficiency be further improved?

In this Letter, we analyze the dynamics and physical mechanisms of ergotropy in model-independent QBs, based on the fact that ergotropy consists of coherent and incoherent components. By means of random or weighted random sampling of quantum states and their associated Hamiltonians [96], we investigate the relationship between the coherent and incoherent contributions on ergotropy and energy-level populations, as well as the impact of quantum resources on both ergotropy components, and the bounds of the ergotropy. We find that both coherence and participation ratio enhance the coherent ergotropy, while diagonal entropy (entanglement) and participation ratio can enhance, remain or suppress the incoherent ergotropy. Additionally, we demonstrate the role of purity in decreasing the locked energy and improving the charging efficiency. We illustrate our major results in the Tavis-Cummings (TC) and Jaynes-Cummings (JC) batteries. These results offer key insights into the design of high-performance QBs, optimizing energy extraction and charging efficiency through quantum resources.

## Preliminaries

We consider the general QB composed by a battery and a charger. The charging process is governed by the following Hamiltonian:

$$H(t) = H_{\mathrm{B}} + H_{\mathrm{C}} + \lambda(t)\mathcal{V}, \tag{1}$$

where $H_{\mathrm{B}}$ and $H_{\mathrm{C}}$ are the Hamiltonians of the battery and charger, respectively. The charging operator $\mathcal{V}$ contains all terms that control energy injection, such as charger-battery interactions and some external

Received 22 January 2026; accepted 24 April 2026; published 1 July 2026
© 2026 Chinese Physical Society and IOP Publishing Ltd. All rights, including for text and data mining, AI training, and similar technologies, are reserved.

Check for updates

driven fields. The time-dependent parameter $\lambda(t)$ describes the charging period, and we assume it follows a step function that equals to 1 for $t \in [0,T]$ and zero elsewhere. At time $t=0$, the charger-battery system is prepared in a product state $\rho_{\rm BC}(0)$ with the battery being the ground state $|\varepsilon_1\rangle$ of $H_{\rm B}$. In a finite time interval $[0,T]$, the evolving state is given by $\rho_{\rm BC}(t) = U(t)\rho_{\rm BC}(0)U^{\dagger}(t)$ with $U(t) = \mathcal{T}\exp[-{\rm i}\int_0^t H(\tau){\rm d}\tau/\hbar]$, where $\mathcal{T}$ is a time-ordering operator. The stored energy in QB at time $t$ is defined by

$$E(\rho_{\rm B}) = {\rm Tr}\left[H_{\rm B}\rho_{\rm B}(t)\right] - {\rm Tr}\left[H_{\rm B}\rho_{\rm B}(0)\right], \tag{2}$$

where $\rho_{\rm B}(t) = {\rm Tr}_{\rm C}\left[\rho_{\rm BC}(t)\right]$ is the reduced density matrix of the battery. The ergotropy is obtained by the difference between the stored energy $E(\rho_{\rm B})$ and locked energy $E(\tilde{\rho}_{\rm B})$

$$\mathcal{E}(\rho_{\rm B}) = {\rm Tr}\left[H_{\rm B}\rho_{\rm B}\right] - {\rm Tr}[H_{\rm B}\widetilde{\rho}_{\rm B}], \tag{3}$$

where $\widetilde{\rho}_{\rm B} = \sum_{n=1}^{d} r_n|\varepsilon_n\rangle\langle\varepsilon_n|$ is the passive state, $r_n$ are the eigenvalues of $\rho_{\rm B}$ ordered as $r_1 \geq r_2 \geq \cdots \geq r_d$, and $|\varepsilon_n\rangle$ are the eigenstates of $H_{\rm B}$ with the corresponding eigenenergies $\varepsilon_n$, which satisfy $\varepsilon_1 \leq \varepsilon_2 \leq \cdots \leq \varepsilon_d$. Here, $d$ denotes the dimension of the battery system. The incoherent ergotropy quantifies the maximum work unitarily extractable from $\rho_{\rm B}$ without altering its coherence and is written as

$$\mathcal{E}_i(\rho_{\rm B}) = {\rm Tr}\{H_{\rm B}\delta_{\rm B}\} - {\rm Tr}\left\{H_{\rm B}\widetilde{\delta}_{\rm B}\right\}, \tag{4}$$

where $\delta_{\rm B} = \sum_{n=1}^{d} p_n|\varepsilon_n\rangle\langle\varepsilon_n|$ is the dephased state of $\rho_{\rm B}$ where $p_n$ denotes the population of $n$th energy level, $\widetilde{\delta}_{\rm B} = \sum_{n=1}^{d} \tilde{p}_n|\varepsilon_n\rangle\langle\varepsilon_n|$ is the passive state of $\delta_{\rm B}$ with $\tilde{p}_n \geq \tilde{p}_{n+1}$. Having defined the incoherent component of $\mathcal{E}$, the coherent contribution to ergotropy can be readily given by the difference

$$\mathcal{E}_c(\rho_{\rm B}) = \mathcal{E}(\rho_{\rm B}) - \mathcal{E}_i(\rho_{\rm B}) = {\rm Tr}\left[\tilde{\delta}_{\rm B}H_{\rm B}\right] - {\rm Tr}\left[\tilde{\rho}_{\rm B}H_{\rm B}\right]. \tag{5}$$

The charging efficiency as another useful quantifier of QBs performance is defined as

$$\mathcal{R}(\rho_{\rm B}) = \frac{\mathcal{E}(\rho_{\rm B})}{E(\rho_{\rm B})}. \tag{6}$$

Quantum coherence and entanglement, the fundamental quantum resources, play an important role in work extraction from quantum systems. The coherence of state $\rho_{\rm B}$ is quantified by the quantum relative entropy of $\rho_{\rm B}$ [1]:

$$C(\rho_{\rm B}) = S_{\rm diag}(\rho_{\rm B}) - S(\rho_{\rm B}), \tag{7}$$

where $S(\rho) = -{\rm Tr}\left[\rho\log(\rho)\right]$ is the von Neumann entropy, and $S_{\rm diag}(\rho_{\rm B}) = -\sum_{n=1}^{d} p_n \log p_n$ is the diagonal entropy. For any pure bipartite state $\rho_{\rm BC}$, the von Neumann entropy of the battery's reduced density matrix $S(\rho_{\rm B})$ characterizes the charger-battery entanglement. When the coherence vanishes, the diagonal entropy equals to the von Neumann entropy, thereby characterizing the entanglement between the battery and charger. To further explore the connection between ergotropy and quantum resources, the participation ratio

$${\rm PR}(\rho_{\rm B}) = \frac{1}{\sum_{n=1}^{d} p_n^2}, \tag{8}$$

a measure of the effective number of occupied states, and purity

$$\mathcal{P}(\rho_{\rm B}) = {\rm Tr}\left[\rho_{\rm B}^2\right], \tag{9}$$

a natural indicator of the mixedness of the battery state, are introduced. These quantities provide a comprehensive framework to assess the interplay between population distribution, quantum resources, and ergotropy in QBs.

## Propositions and Examples

*Proposition* 1. In the absence of population inversion, the ergotropy coincides with the coherent ergotropy–with the incoherent ergotropy being zero–i.e., $\mathcal{E} = \mathcal{E}_c$, $\mathcal{E}_i = 0$. In the presence of population inversion, however, the ergotropy is governed by both coherent and incoherent contributions, such that $\mathcal{E} = \mathcal{E}_c + \mathcal{E}_i$.

Population evolution plays a crucial role in the charging process, which is generally accompanied by population changes and inversion. As sketched in Fig. 1(a), the charging process can usually be divided into three distinct cases or stages: (I) The no population inversion, where the population is ordered in a descending sort, i.e., $\forall\ 1 \leq n < m \leq d$, $p_n \geq p_m$; (II) The local population inversion, characterized by the population inversion involving some energy levels, i.e., $\exists\ 1 \leq n < m \leq d$, $p_n < p_m$; (III) The global population inversion, where the population is ordered in an ascending sort, i.e., $\forall\ 1 \leq n < m \leq d$, $p_n \leq p_m$ and $p_1 < p_d$. Here, $t_1$ and $t_2$ denote the critical times at which the system enters the local and global population inversion stages, respectively. For two-level QBs, the process only involves two stages, namely I and III.

According to Eq. (4), the incoherent ergotropy is given by $\mathcal{E}_i(\rho_{\rm B}) = \sum_{n=1}^{d}(p_n - \tilde{p}_n)\varepsilon_n$. In the absence of population inversion, $p_n = \tilde{p}_n$ for all $n$, so that the incoherent ergotropy vanishes, $\mathcal{E}_i = 0$, and the total ergotropy reduces to its coherent part, namely, $\mathcal{E} = \mathcal{E}_c$. Conversely, in the stage of local or global population inversion, there exists at least one pair of populations satisfying $p_m > p_n$ with $m > n$, which contributes positively through $(p_m - p_n)(\varepsilon_m - \varepsilon_n) > 0$; therefore, the incoherent ergotropy is nonvanishing, and the total ergotropy is given by $\mathcal{E} = \mathcal{E}_c + \mathcal{E}_i$.

In Figs. 1(b)–1(d), we illustrate the above results in two-level and three-level QBs (it remains valid in the high-dimensional case). Here, we normalize the Hamiltonian of battery as $1/(\varepsilon_d - \varepsilon_1)[2H_{\rm B} - (\varepsilon_d + \varepsilon_1)\mathbb{I}] \to H_{\rm B}$ [97]. In the stage with no population inversion corresponding to the region I, the coherent part governs the ergotropy. In the local population inversion depicted in the region II, both incoherent and coherent ergotropy jointly control the ergotropy, whereas in the global population inversion corresponding to the region III, the incoherent part gradually becomes dominant as the populations of higher-energy levels increase. Until the population of the highest energy level $p_2$ in Fig. 1(b) or $p_3$ in Figs. 1(c) and 1(d) reaches 1, the ergotropy is consistent with the incoherent ergotropy. Furthermore, we obtain an important corollary: the lower bound of ergotropy is the incoherent ergotropy, and the upper bound is the stored energy of battery for any given population distribution, i.e., $\mathcal{E}_{\rm min} = \mathcal{E}_i = \sum_{n=1}^{d}(p_n - \tilde{p}_n)\varepsilon_n$, $\mathcal{E}_{\rm max} = E = \sum_{n=1}^{d} p_n\varepsilon_n - \varepsilon_1$. In the model-independent framework, these bounds are determined by the populations and the energy levels of $H_{\rm B}$.

This proposition reveals the dynamical feature of ergotropy from perspective of coherent and incoherent contributions. It shows that population inversion is both a necessary condition for nonzero incoherent ergotropy and a threshold at which ergotropy changes from purely coherent to containing both coherent and incoherent components. A natural question arises: what is the physical mechanism underlying the coherent and incoherent ergotropy, i.e., which quantum resources or factors influence the coherent and incoherent parts?

*Proposition* 2. (i) The coherent ergotropy–enhanced by both coherence and participation ratio–exhibits well-defined upper and lower bounds, which correspond to the maximally delocalized state and pure state limits, respectively. (ii) The incoherent ergotropy–being enhanced, maintained, or suppressed–depends on the diagonal entropy or participation ratio, and the ordering of level populations. For each ordering, there exist upper and lower bounds of the incoherent ergotropy, as well as a series of special points of the diagonal entropy $\log n$: extremum and corner points, across which the boundary behavior of the incoherent ergotropy may change.

To explore the roles of coherent and incoherent factors on the coherent ergotropy, we characterize the coherent and incoherent factors as coherence and participation ratio, respectively. We first investigate the effect of the coherence and participation ratio on the coherent ergotropy through a large sample of randomly generated states on a single randomly generated $H_{\rm B}$. To achieve uniform random sampling over the state space, we introduce the Hilbert–Schmidt distance, which naturally induces the Hilbert–Schmidt volume measure [98]. Sampling from the Hilbert–Schmidt measure assigns probabilities

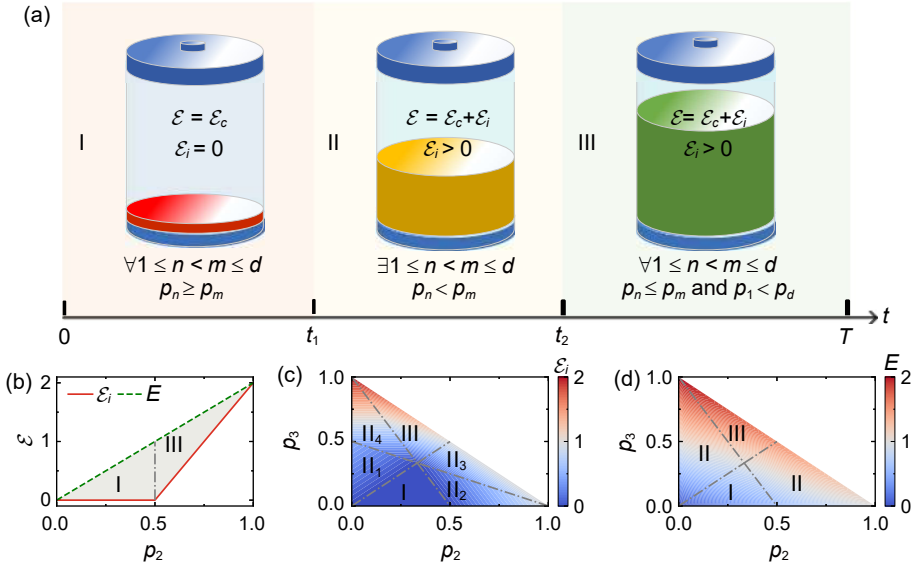


**Fig. 1.** (a) Schematic diagram of the charging process, which consists of three stages: Stage I, no population inversion; Stage II, local population inversion; Stage III, global population inversion. The other parameters satisfy $0 \le t_1 \le t_2 \le T$ and $T > 0$. (b) The ergotropy as a function of the excited energy level population $p_2$ for two-level QBs. (c) and (d) The incoherent ergotropy and the stored energy as a function of the population of 2th and 3th energy level, $p_2, p_3$ for three-level QBs. As shown in panel (c), the region of local population inversion contains different population ordering: In $\mathrm{II}_1$, the population ordering is $p_1 \ge p_3 > p_2$; in $\mathrm{II}_2$, $p_2 > p_1 \ge p_3$; in $\mathrm{II}_3$, $p_2 > p_3 \ge p_1$ or $p_2 \ge p_3 > p_1$; and in $\mathrm{II}_4$, $p_3 \ge p_1 > p_2$ or $p_3 > p_1 \ge p_2$. Here, the Hamiltonian $H_\mathrm{B}$ has equally spaced energy levels for two-level and three-level QBs.

proportional to the Hilbert–Schmidt volumes of regions in the state space. Numerically, this sampling can be realized through a complex Ginibre random matrix $G$, $\rho = GG^\dagger/\mathrm{Tr}[GG^\dagger]$ [99]. The convergence of this random sampling method is confirmed by examining the empirical distribution and cumulative means of the relevant observables. In all calculations, we generate the enough sample sizes to ensure the convergence. Within a model-independent framework, the battery Hamiltonian is sampled as generally as possible, which requires the $d^2$ real parameters to be statistically independent and the sampling measure to be invariant under unitary transformation. There requirements uniquely lead to the Gaussian unitary ensemble. Specifically, the Hamiltonian can be generated as $H = (G + G^\dagger)/(2)$ [100]. The details are provided in Supplemental Material (SM). The results are illustrated in Figs. 2(a) and 2(b), which reveal a positive dependence of coherent ergotropy on the coherence and participation ratio. For a given coherence, a larger participation ratio generally indicates a higher locked energy $\mathrm{Tr}\left[\tilde{\delta}_\mathrm{B} H_\mathrm{B}\right]$ of the dephased state $\delta_\mathrm{B}$ and thereby enhancing the coherent ergotropy (as detailed in SM); for a given participation ratio, a greater coherence implies higher purity of $\rho_\mathrm{B}$ and the lower locked energy $\mathrm{Tr}\left[\tilde{\rho}_\mathrm{B} H_\mathrm{B}\right]$ (see also Proposition 3), which likewise contributes to increased coherent ergotropy. In particular, for two-level QBs, we also present analytical results of coherent ergotropy as a function of both coherence and participation ratio in the SM, and prove the positive dependence of coherent ergotropy on the coherence and participation ratio.

Due to that the participation ratio of the pure state $\rho_\mathrm{B}^\mathrm{pur}$ is minimal and that of the completely delocalized state $\rho_\mathrm{B}^\mathrm{deloc}$ (meaning its energy-level populations satisfy $p_n = 1/d$ [101]) is maximal for any given coherence, we can obtain the bounds for coherent ergotropy $\mathcal{E}_c$:

$$\mathcal{E}_c^L(\rho_\mathrm{B}^\mathrm{pur}) \le \mathcal{E}_c(\rho_\mathrm{B}) \le \mathcal{E}_c^U(\rho_\mathrm{B}^\mathrm{deloc}), \tag{10}$$

where $\mathcal{E}_c^L(\rho_\mathrm{B}^\mathrm{pur}) = \sum_{n=1}^d \tilde{p}_n(\varepsilon_n - \varepsilon_1)$ and $\mathcal{E}_c^U(\rho_\mathrm{B}^\mathrm{deloc}) = \sum_{n=1}^d (1/d - r_n)\varepsilon_n$ represent the lower and upper bounds of coherent ergotropy, respectively. These bounds are given by the minimum coherent ergotropy over all pure states, i.e., $\mathcal{E}_c^L(\rho_\mathrm{B}^\mathrm{pur}) = \min \mathcal{E}_c(\rho_\mathrm{B}^\mathrm{pur})$, and by the maximum coherent ergotropy over all completely delocalized states, i.e., $\mathcal{E}_c^U(\rho_\mathrm{B}^\mathrm{deloc}) = \max \mathcal{E}_c(\rho_\mathrm{B}^\mathrm{deloc})$, respectively. The lower bound corresponds to the pure state with populations arranged in descending order, which satisfy $\tilde{p}_n = \exp(-\beta_l(\varepsilon_n - \varepsilon_1))/Z_l$ with the inverse temperature $\beta_l$ and the partition function $Z_l = \sum_{n=1}^d \exp(-\beta_l(\varepsilon_n - \varepsilon_1))$. The upper bound corresponds to the completely delocalized state characterized by eigenvalues $r_n = \exp(-\beta_u \varepsilon_n)/Z_u$ with the inverse temperature $\beta_u$ and the partition function $Z_u = \sum_{n=1}^d \exp(-\beta_u \varepsilon_n)$. Moreover, in comparison to the bounds in Ref. [17], our bounds are tighter at the high coherence case. For clarity of presentation, the detailed derivation of the bounds is obtained in the SM.

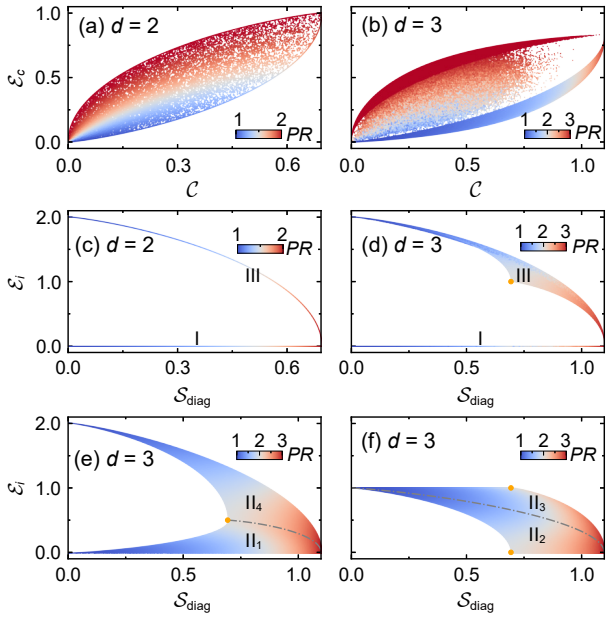


**Fig. 2.** (a) and (b) The coherent ergotropy $\mathcal{E}_c$ as a function of the coherence $C$ and participation ratio $PR$ for randomly sampled states $\rho_\mathrm{B}$, Hamiltonian $H_\mathrm{B}$ for two-level and three-level QBs. Here, the Hamiltonian $H_\mathrm{B}$ is normalized. (c)–(f) For the cases of the no, local and global population inversion the incoherent ergotropy as a function of the diagonal entropy and participation ratio for randomly sampled states $\rho_\mathrm{B}$ and Hamiltonian $H_\mathrm{B}$. The symbols I, $\mathrm{II}_1$, $\mathrm{II}_2$, $\mathrm{II}_3$, $\mathrm{II}_4$ and III denote the same configurations as in Fig. 1(c). The orange dots in (e) and (f) correspond to the value of diagonal entropy, $\log 2$. We focus on Hamiltonians with equally spaced and normalized energy levels. Panel (a) contains $10^5$ randomly sampled states, while (b)–(f) together contain $10^7$ states.

We now turn to the incoherent ergotropy. Since the incoherent ergotropy is governed solely by incoherent factors, we investigate the effects of diagonal entropy and participation ratio on the incoherent ergotropy through the weighted random sampling of $\rho_{\mathrm{B}}$ and $H_{\mathrm{B}}$, as shown in Figs. 2(c)–2(f) for two- and three-levels QBs. Based on the Hilbert–Schmidt sampling scheme, we supplement the random density matrices in the low-diagonal-entropy regime (see SM for details). According to Proposition 1, the incoherent ergotropy remains zero in the absence of population inversion [see also Figs. 1(b) and 1(c)]. We mainly focus on the cases of the global and local population inversion. For the two-level QBs, the incoherent ergotropy is negatively related to the diagonal entropy or participation ratio in the case of global population inversion, as depicted in Fig. 2(c). For the three-level QBs, the relationship between the incoherent ergotropy and the diagonal entropy or participation ratio is no longer monotonic; it may increase, remain, or suppress under different conditions (for example, when the variation of energy-level population satisfies $\Delta p_1 > \max\{-1/2\Delta p_2, -\Delta p_2 \log(p_3/p_2)/\log(p_3/p_2)\}$ or $\Delta p_1 < \min\{-1/2\Delta p_2, -\Delta p_2 \log(p_3/p_2)/\log(p_3/p_2)\}$, the diagonal entropy suppresses the incoherent ergotropy). We provide the detailed proof of these conditions in SM. Nevertheless, its bounds remain negatively related with the diagonal entropy (participation ratio). Therefore, to achieve larger incoherent ergotropy, smaller diagonal entropy or participation ratio is generally preferred in the case of global population inversion. For the case of the local population inversion, the relation is similar to that for global population inversion. For each ordering, the incoherent ergotropy has upper and lower bounds, as well as extremum and corner points of the diagonal entropy. An extremum point refers to a point on the boundary of incoherent ergotropy where a physical quantity attains a local maximum or minimum, corresponding to $S_{\mathrm{diag}} = 0$ and $S_{\mathrm{diag}} = \log d$, respectively. When $\mathcal{S}_{\mathrm{diag}} = 0$, $\rho_{\mathrm{B}}$ is localized in an arbitrary eigenstate $|\varepsilon_n\rangle$, i.e., $\mathcal{E}_i = \varepsilon_n - \varepsilon_1$; when $\mathcal{S}_{\mathrm{diag}} = \log d$, the population is equally distributed across all energy levels in $H_{\mathrm{B}}$, i.e., $\mathcal{E}_i = 0$. A corner point is defined as a continuous but not smooth point on the boundary of incoherent ergotropy. Such points typically appear at diagonal entropy $\log n$ (with $n = 2, 3, ..., d-1$), across which the boundary behavior changes. For example, in $\mathrm{II}_2$ region of Fig. 2(e), before the corner point, the upper bound of incoherent ergotropy increases with the diagonal entropy, while after the corner point, it is suppressed.

This proposition reveals the intrinsic relationship between coherent ergotropy and both coherence and the participation ratio, while linking incoherent ergotropy to diagonal entropy, the participation ratio, and the ordering of energy-level populations. Not only ergotropy but also charging efficiency should be considered to fully assess QB performance. Given that the stored energy can be fully extracted in the pure state, a natural question arises as to whether increasing purity enhances the charging efficiency.

*Proposition* 3. Purity generally suppresses the locked energy $\mathrm{Tr}\left[\tilde{\rho}_{\mathrm{B}} H_{\mathrm{B}}\right]$ while it enhances the charging efficiency $\mathcal{R}$ (in the presence of population inversion) during the charging process.

For energy storage devices, the charging efficiency represents another crucial performance metric. To realize high-performance QBs, we now explore how purity can be utilized to reduce the locked energy and enhance the charging efficiency. The purity of $\rho_{\mathrm{B}}$ remains invariant under unitary evolution: $\mathcal{P}(\rho_{\mathrm{B}}) = \mathrm{Tr}[\rho_{\mathrm{B}}^2] = \mathrm{Tr}[U\rho_{\mathrm{B}}U^\dagger U\rho_{\mathrm{B}}U^\dagger] = \mathrm{Tr}[\tilde{\rho}_{\mathrm{B}}^2] = \sum_{n=1}^{d} r_n^2$. For the passive state $\tilde{\rho}_{\mathrm{B}}$, the purity and participation ratio satisfy $\mathcal{P}(\tilde{\rho}_{\mathrm{B}}) = 1/\mathrm{PR}(\tilde{\rho}_{\mathrm{B}})$. This implies that an increase in purity of $\rho_{\mathrm{B}}$ enhances the localization of $\tilde{\rho}_{\mathrm{B}}$. Due to $r_1 \geq r_2 \geq \cdots \geq r_d$, stronger localization increases the population of $\tilde{\rho}_{\mathrm{B}}$ in lower energy levels, thereby reducing locked energy $E(\tilde{\rho}_{\mathrm{B}})$. Since the charging efficiency is given by $\mathcal{R}(\rho_{\mathrm{B}}) = 1 - E(\tilde{\rho}_{\mathrm{B}})/E(\rho_{\mathrm{B}})$, a decrease in the locked energy may enhance the charging efficiency. Figure 3 illustrates the dependence of both the locked energy and the charging efficiency (under population inversion) on purity of two- and three-levels QBs, based on a large sample of randomly generated states on a single randomly generated Hamiltonian. The random states are generated by constructing the eigenvalue with a target purity and then applying unitary matrices sampled from the Haar measure, thereby obtaining the state with the desired purity (see SM for details). Purity typically suppresses the locked energy, particularly in the two-level QBs where the locked energy is negatively related to the purity [see Figs. 3(a) and 3(b)]. In addition, purity generally enhances the charging efficiency, as observed for each population ordering in the two- and three-level QBs [see Figs. 3(c) and 3(d)]. Notably, when the battery is in a pure state, i.e., $\mathcal{P}(\rho_{\mathrm{B}}) = 1$, the charging efficiency reaches its maximum value 1, indicating that the stored energy in the battery can be fully extracted. Consequently, increasing the purity can enable higher charging efficiency. Since we focus on a model-independent framework, the propositions apply to arbitrary chargers and charging protocols, and also hold for higher-dimensional QBs with arbitrary energy-level spacings.

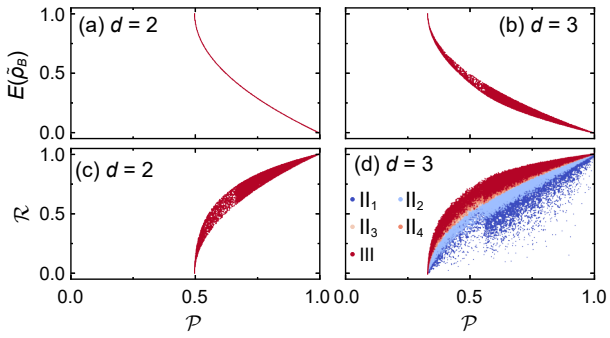


**Fig. 3.** The dependence of both (a) and (b) the locked energy $E(\tilde{\rho}_{\mathrm{B}})$ and (c) and (d) the charging efficiency $\mathcal{R}$ on purity $\mathcal{P}$ for two-level and three-level QBs. As shown in panel (d), the symbols $\mathrm{II}_1$, $\mathrm{II}_2$, $\mathrm{II}_3$, $\mathrm{II}_4$, and III denote the same configurations as in Fig. 1(c). Here, the Hamiltonian $H_{\mathrm{B}}$ is normalized. Each panel contains $10^5$ randomly sampled states.

*Example: JC battery and TC battery.* The TC battery consists of $N_{\mathrm{B}}$ two-level atoms and a single-mode cavity. The charger-battery system can be described by the following Hamiltonian (we set $\hbar = 1$)

$$H = \omega_{\mathrm{c}} a^\dagger a + \omega_{\mathrm{b}} J_z + g(J_+ a + J_- a^\dagger), \tag{11}$$

where $H_{\mathrm{C}} = \omega_{\mathrm{c}} a^\dagger a$, $H_{\mathrm{B}} = \omega_{\mathrm{b}} J_z$, and $\mathcal{V} = g(J_+ a + J_- a^\dagger)$ are the Hamiltonian of charger, battery and their interaction, respectively. The $a$ ($a^\dagger$) annihilates (creates) a photon in cavity with frequency $\omega_{\mathrm{c}}$ and $g$ characterizes the strength of coupling. Here, $J_\alpha = 1/2 \sum_{n=1}^{N_{\mathrm{B}}} \sigma_n^\alpha$ ($\alpha = x, y, z$) is a collective spin operator and $J_\pm = J_x \pm \mathrm{i} J_y$ are spin ladder operators. We consider the resonant scenario, i.e., $\omega_{\mathrm{c}} = \omega_{\mathrm{b}} = \omega$. When the number of two-level atom is one, the Hamiltonian (11) can describe the JC battery. The initial state of system is the product state $|\psi(0)\rangle = |0\rangle_{\mathrm{B}} \otimes |\alpha\rangle_{\mathrm{C}}$, where the battery is in the ground state of $H_{\mathrm{B}}$, i.e., $|0\rangle_{\mathrm{B}} = |\downarrow, \ldots, \downarrow\rangle$ and the charger is in a coherent state $|\alpha\rangle_{\mathrm{C}} = \sum_n \alpha_n |n\rangle_{\mathrm{C}}$ with $N_{\mathrm{c}}$ photons.

Time evolution of ergotropy, coherent ergotropy and incoherent ergotropy are shown in Figs. 4(a) and 4(b) for JC battery and TC battery, respectively. Combining the energy level populations of JC battery and TC battery [see Figs. 4(c) and 4(d)], it supports the Proposition 1 that $\mathcal{E} = \mathcal{E}_c$, $\mathcal{E}_i = 0$ without the population inversion and $\mathcal{E} = \mathcal{E}_c + \mathcal{E}_i$ with the population inversion. For JC QB, the upper bound of ergotropy is quantified by $\mathcal{E}_{\max} = \hbar\omega/2\left[1 - \sum_n |\alpha_n|^2 \cos(\Omega_n t)\right]$ with $\Omega_n = 2g\sqrt{n}$. The lower bound is given by $\mathcal{E}_{\min}(t) = -\hbar\omega \sum_n |\alpha_n|^2 \cos\Omega_n t$ for $p_2 > p_1$, and $\mathcal{E}_{\min}(t) = 0$ otherwise, where $p_1 = \sum_n |\alpha_n|^2 \sin^2(\Omega_n t/2)$ and $p_2 = \sum_n |\alpha_n|^2 \cos^2(\Omega_n t/2)$ are the ground- and excited-state populations, respectively. Further, we demonstrate the influence of quantum resource (quantum coherence, diagonal entropy and participation ratio) on both the coherent ergotropy and incoherent ergotropy in Figs. 4(a), 4(b), 4(e), and 4(f). The coherent ergotropy increases with the coherence and participation ratio. The incoherent ergotropy can be enhanced and suppressed by the diagonal entropy or participation ratio. In the case of global population inversion (the III region), for JC and TC batteries the incoherent ergotropy is negatively related to the diagonal entropy or participation ratio and the maximal value of incoherent ergotropy

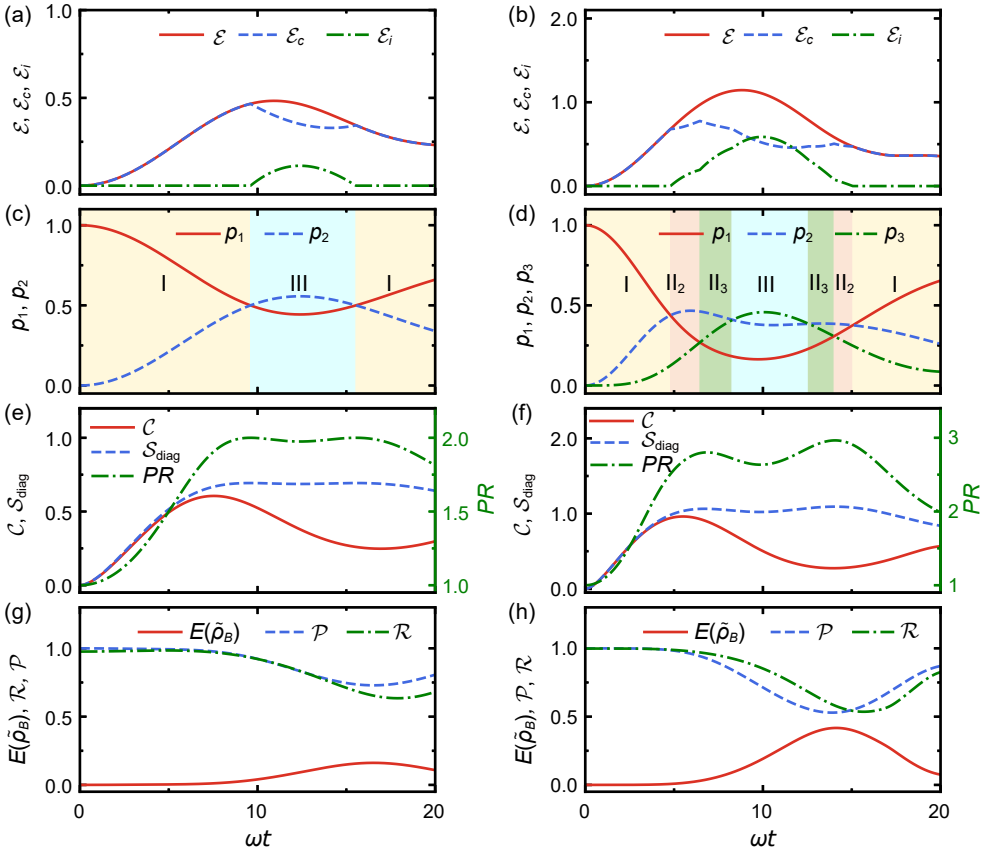


**Fig. 4.** Time evolution of (a) and (b) ergotropy, coherent ergotropy, incoherent ergotropy, (c) and (d) energy level populations, (e) and (f) coherence, diagonal entropy, participation ratio, (g) and (h) locked energy, purity and charging efficiency. (a), (c), (e), and (g) correspond to the case of JC QBs, and (b), (d), (f), and (h) correspond to the case of TC QBs containing two atoms ($N_{\rm B} = 2$), which is analogous to the three-level QBs. The symbols I, II$_2$, II$_3$, III denote the same setting as in Fig. 1(c). Other parameters are set to $\omega = 1$, $g = 0.1$, and $N_{\rm c} = N_{\rm B}$.

corresponds to the minimal value of the diagonal entropy or participation ratio. In case of local population inversion (the II$_2$ region), the diagonal entropy enhances the incoherent ergotropy. In addition, the dependence of both the locked energy and the charging efficiency on the purity is illustrated in Figs. 4(g) and 4(h). It is evident that the purity suppresses the locked energy and enhances the charging efficiency. For TC QBs with larger $N_{\rm B}$, namely, with more complex energy level structures, the relation between charging efficiency and purity remains unchanged, while the charging efficiency is enhanced with increasing $N_{\rm B}$ (see SM for details). For JC QBs with the charger initially prepared in a Fock states and the open Dicke QBs in SM, the above results still hold.

## Conclusions

We have demonstrated the coherent and incoherent contributions on ergotropy and the impact of quantum resource on them for general QBs based on the energy level populations. During the charging process, the ergotropy coincides with the coherent ergotropy in the absence of population inversion and is determined by both the coherent and incoherent ergotropy in the presence of population inversion. For any given population, the lower bound of ergotropy is the incoherent ergotropy, and its upper bound is the stored energy. The coherence and participation ratio jointly can enhance the coherent ergotropy, whose upper and lower bounds are attained for the maximally delocalized state and the pure state, respectively. The diagonal entropy and participation ratio can enhance, remain or suppress the incoherent ergotropy under different conditions. In the cases of global population inversion, the diagonal entropy (participation ratio) generally suppresses the incoherent ergotropy and the minimal value of diagonal entropy (participation ratio) corresponds to the maximal value of the incoherent ergotropy. We have also illustrated that the purity generally can suppress the locked energy and enhance the charging efficiency. Our results elucidate a clear ergotropy mechanism in general QBs and provide a valuable guidance for optimal ergotropy and charging efficiency of QBs, advancing high-performance quantum energy-storage devices.

## Acknowledgements

The work is supported by the National Natural Science Foundation of China (Grant No. 12475026) and the Natural Science Foundation of Gansu Province (Grant No. 25JRRA799).

## References

[1] Baumgratz T, Cramer M, and Plenio M B 2014 *Phys. Rev. Lett.* **113** 140401
[2] Streltsov A, Adesso G, and Plenio M B 2017 *Rev. Mod. Phys.* **89** 041003
[3] Designolle S, Uola R, Luoma K, and Brunner N 2021 *Phys. Rev. Lett.* **126** 220404
[4] Yao Y, Xiao X, Ge L, and Sun C P 2015 *Phys. Rev. A* **92** 022112
[5] Horodecki R, Horodecki P, Horodecki M, and Horodecki K 2009 *Rev. Mod. Phys.* **81** 865
[6] Giraldi F and Grigolini P 2001 *Phys. Rev. A* **64** 032310
[7] Życzkowski K, Horodecki P, Horodecki M, and Horodecki R 2001 *Phys. Rev. A* **65** 012101
[8] Zanardi P 2001 *Phys. Rev. A* **63** 040304
[9] Brandão F, Horodecki M, Ng N, Oppenheim J, and Wehner S 2015 *Proc. Natl. Acad. Sci.* **112** 3275
[10] Ćwikliński P, Studziński M, Horodecki M, and Oppenheim J 2015 *Phys. Rev. Lett.* **115** 210403

[11] Allahverdyan A E, Balian R, and Nieuwenhuizen T M 2004 *EPL* **67** 565
[12] Šafránek D, Rosa D, and Binder F C 2023 *Phys. Rev. Lett.* **130** 210401
[13] Castellano R, Farina D, Giovannetti V, and Acin A 2024 *Phys. Rev. Lett.* **133** 150402
[14] Salvia R, De Palma G, and Giovannetti V 2023 *Phys. Rev. A* **107** 012405
[15] Francica G, Goold J, Plastina F, and Paternostro M 2017 *npj Quantum Inf.* **3** 12
[16] Niu Z, Wu Y, Wang Y, Rong X, and Du J 2024 *Phys. Rev. Lett.* **133** 180401
[17] Francica G, Binder F C, Guarnieri G, Mitchison M T, Goold J, and Plastina F 2020 *Phys. Rev. Lett.* **125** 180603
[18] Alicki R and Fannes M 2013 *Phys. Rev. E* **87** 042123
[19] Campaioli F, Gherardini S, Quach J Q, Polini M, and Andolina G M 2024 *Rev. Mod. Phys.* **96** 031001
[20] Quach J, Cerullo G, and Virgili T 2023 *Joule* **7** 2195
[21] Campaioli F, Pollock F A, and Vinjanampathy S 2018 *Thermodynamics in the Quantum Regime*, edited by Binder F, Correa L, Gogolin C, Anders J, and Adesso G (Springer, Cham) p. 207
[22] Khan N A, Zhang X, Huang C, Liu Y, and He D 2025 *Phys. Rev. B* **112** 104318
[23] Wang Y, Wu H, and Zhao Q 2025 *Phys. Rev. A* **112** L030201
[24] Lu Z G, Tian G, Lü X Y, and Shang C 2025 *Phys. Rev. Lett.* **134** 180401
[25] Rojo-Francas A, Isaule F, Santos A C, JuliaDiaz B, and Zinner N T 2024 *Phys. Rev. A* **110** 032205
[26] Zhang D, Ma S, Jiang Y, Yu Y, Jin G, and Chen A 2024 *Phys. Rev. A* **110** 032211
[27] Joshi J and Mahesh T S 2022 *Phys. Rev. A* **106** 042601
[28] Ferraro D, Campisi M, Andolina G M, Pellegrini V, and Polini M 2018 *Phys. Rev. Lett.* **120** 117702
[29] Andolina G M, Farina D, Mari A, Pellegrini V, Giovannetti V, and Polini M 2018 *Phys. Rev. B* **98** 205423
[30] Andolina G M, Keck M, Mari A, Giovannetti V, and Polini M 2019 *Phys. Rev. B* **99** 205437
[31] Rossini D, Andolina G M, and Polini M 2019 *Phys. Rev. B* **100** 115142
[32] Santos A C, Çakmak B, Campbell S, and Zinner N T 2019 *Phys. Rev. E* **100** 032107
[33] Rossini D, Andolina G M, Rosa D, Carrega M, and Polini M 2020 *Phys. Rev. Lett.* **125** 236402
[34] Peng L, He W B, Chesi S, Lin H Q, and Guan X W 2021 *Phys. Rev. A* **103** 052220
[35] Dou F Q, Wang Y J, and Sun J A 2020 *EPL* **131** 43001
[36] Dou F Q, Wang Y J, and Sun J A 2021 *Front. Phys.* **17** 31503
[37] Santos A C, Saguia A, and Sarandy M S 2020 *Phys. Rev. E* **101** 062114
[38] Qi S F and Jing J 2021 *Phys. Rev. A* **104** 032606
[39] Konar T K, Lakkaraju L G C, Ghosh S, and Sen(De) A 2022 *Phys. Rev. A* **106** 022618
[40] Ghosh S, Chanda T, and Sen(De) A 2020 *Phys. Rev. A* **101** 032115
[41] Song M L, Li L J, Song X K, Ye L, and Wang D 2022 *Phys. Rev. E* **106** 054107
[42] Rodríguez R R, Ahmadi B, Mazurek P, Barzanjeh S, Alicki R, and Horodecki P 2023 *Phys. Rev. A* **107** 042419
[43] Dou F Q, Lu Y Q, Wang Y J, and Sun J A 2022 *Phys. Rev. B* **105** 115405
[44] Dou F Q and Yang F M 2023 *Phys. Rev. A* **107** 023725
[45] Guo W X, Yang F M, and Dou F Q 2024 *Phys. Rev. A* **109** 032201
[46] Song W L, Liu H B, Zhou B, Yang W L, and An J H 2024 *Phys. Rev. Lett.* **132** 090401
[47] Grazi R, Sacco Shaikh D, Sassetti M, Traverso Ziani N, and Ferraro D 2024 *Phys. Rev. Lett.* **133** 197001
[48] Downing C A and Ukhtary M S 2023 *Commun. Phys.* **6** 322
[49] Wang L, Liu S Q, Wu F l, Fan H, and Liu S Y 2024 *Phys. Rev. A* **110** 062204
[50] Canzio A, Cavina V, Polini M, and Giovannetti V 2025 *Phys. Rev. A* **111** 022222
[51] Li L, Zhao S L, Shi Y H, Chen B J, Ruan X, Liang G H, Yuan W P, Song J C, Deng C L, Liu Y, Li T M, Liu Z H, Guo X Y, Song X, Xu K, Fan H, Xiang Z, and Zheng D 2025 *Phys. Rev. Appl.* **24** 054033
[52] Campaioli F, Pollock F A, Binder F C, Céleri L, Goold J, Vinjanampathy S, and Modi K 2017 *Phys. Rev. Lett.* **118** 150601
[53] Zhang Y Y, Yang T R, Fu L, and Wang X 2019 *Phys. Rev. E* **99** 052106
[54] Ma H B, Xu K, Li H G, Li Z G, and Zhu H J 2024 *Phys. Rev. A* **110** 022433
[55] Kamin F H, Salimi S, and Arjmandi M B 2024 *Phys. Rev. A* **109** 022226
[56] Downing C A and Ukhtary M S 2024 *Phys. Rev. A* **109** 052206
[57] Arjmandi M B, Mohammadi H, and Santos A C 2022 *Phys. Rev. E* **105** 054115
[58] Xu K, Li H G, Li Z G, Zhu H J, Zhang G F, and Liu W M 2022 *Phys. Rev. A* **106** 012425
[59] Seah S, Perarnau-Llobet M, Haack G, Brunner N, and Nimmrichter S 2021 *Phys. Rev. Lett.* **127** 100601
[60] Erdman P A, Andolina G M, Giovannetti V, and Noé F 2024 *Phys. Rev. Lett.* **133** 243602
[61] Medina I, Culhane O, Binder F C, Landi G T, and Goold J 2025 *Phys. Rev. Lett.* **134** 220402
[62] Fasihi M A, Jafarzadeh Bahrbeig R, Mojaveri B, and Haji Mohammadzadeh R 2025 *Phys. Rev. E* **112** 024117
[63] Cristiano C, Viotti L, and Villar P I 2025 *Phys. Rev. A* **112** 062234
[64] Canzio A, Cavina V, Menta R, and Giovannetti V 2025 arXiv: 2509.08899 [quant-ph]
[65] Sarkar A, Chaki P, Ghosh P, and Sen U 2025 arXiv: 2505.16851 [quant-ph]
[66] Grazi R, Johannesson H, Ferraro D, and Ziani N T 2025 arXiv: 2512.14521 [quant-ph]
[67] Zhang D, Ma S, Yu Y, Jin G, and Chen A 2025 *Adv. Quantum Technol.* **8** e2500243
[68] Crescente A, Carrega M, Sassetti M, and Ferraro D 2020 *Phys. Rev. B* **102** 245407
[69] Santos T F F, de Almeida Y V, and Santos M F 2023 *Phys. Rev. A* **107** 032203
[70] Ahmadi B, Mazurek P, Horodecki P, and Barzanjeh S 2024 *Phys. Rev. Lett.* **132** 210402
[71] Zhu G, Chen Y, Hasegawa Y, and Xue P 2023 *Phys. Rev. Lett.* **131** 240401
[72] Lai P R, Lin J D, Huang Y T, Jan H C, and Chen Y N 2024 *Phys. Rev. Res.* **6** 023136
[73] Gherardini S, Campaioli F, Caruso F, and Binder F C 2020 *Phys. Rev. Res.* **2** 013095
[74] Arjmandi M B, Shokri A, Faizi E, and Mohammadi H 2022 *Phys. Rev. A* **106** 062609
[75] Gyhm J Y and Fischer U R 2024 *AVS Quantum Sci.* **6** 012001
[76] Tirone S, Salvia R, Chessa S, and Giovannetti V 2025 *Phys. Rev. A* **111** 012204
[77] Garcia-Pintos L P, Hamma A, and del Campo A 2020 *Phys. Rev. Lett.* **125** 040601
[78] Song M L, Song X K, Ye L, and Wang D 2024 *Phys. Rev. E* **109** 064103
[79] Tirone S, Salvia R, Chessa S, and Giovannetti V 2023 *Phys. Rev. Lett.* **131** 060402
[80] Kamin F H, Tabesh F T, Salimi S, and Santos A C 2020 *Phys. Rev. E* **102** 052109
[81] Shi H L, Ding S, Wan Q K, Wang X H, and Yang W L 2022 *Phys. Rev. Lett.* **129** 130602
[82] Simon R P A, Anders J, and Hovhannisyan K V 2025 *Phys. Rev. Lett.* **134** 010408
[83] Ali A, Al-Kuwari S, Hussain M I, Byrnes T, Rahim M T, Quach J Q, Ghominejad M, and Haddadi S 2024 *Phys. Rev. A* **110** 052404
[84] Monsel J, Fellous-Asiani M, Huard B, and Auffèves A 2020 *Phys. Rev. Lett.* **124** 130601
[85] Çakmak B 2020 *Phys. Rev. E* **102** 042111
[86] Shokri A, Faizi E, and Arjmandi M B 2025 *Phys. Rev. E* **111** 064117
[87] Yang S, Hu W, Tian J, He Z, and Qiu L 2025 *Quantum Inf. Process.* **24** 225
[88] Yang D L, Yang F M, and Dou F Q 2024 *Phys. Rev. B* **109** 235432
[89] Andolina G M, Keck M, Mari A, Campisi M, Giovannetti V, and Polini M 2019 *Phys. Rev. Lett.* **122** 047702
[90] Li L, Zhao S, Shi Y H, Xu K, Fan H, Zheng D, and Xiang Z 2025 *Phys. Rev. Res.* **7** 043236

[91] Song W L, Wang J L, Zhou B, Yang W L, and An J H 2025 *Phys. Rev. Lett.* **135** 020405
[92] Yang X, Yang Y H, Alimuddin M, Salvia R, Fei S M, Zhao L M, Nimmrichter S, and Luo M X 2023 *Phys. Rev. Lett.* **131** 030402
[93] Caravelli F, Yan B, García-Pintos L P, and Hamma A 2021 *Quantum* **5** 505
[94] Li Y F, He S R, Ouyang P H, Feng X N, and Wei L F 2025 *Phys. Rev. A* **112** 022217
[95] Yao Y and Shao X Q 2025 *Phys. Rev. A* **111** 062616
[96] Hokkyo A and Ueda M 2025 *Phys. Rev. Lett.* **134** 010406
[97] Konar T K, Lakkaraju L G C, and Sen (De) A 2024 *Phys. Rev. A* **109** 042207
[98] Bengtsson I and Zyczkowski K 2006 *Geometry of Quantum States: An Introduction to Quantum Entanglement* (Cambridge University Press) p. 347
[99] Zyczkowski K and Sommers H J 2001 *J. Phys. A* **34** 7111
[100] Edelman A and Rao N R 2005 *Acta Numerica.* **14** 233
[101] Karamlou A H, Braumüller J, Yanay Y *et al*. 2022 *npj Quantum Inf.* **8** 35